

### doi:10.1016/S0360-3016(02)04514-5

#### PHYSICS CONTRIBUTION

# A THREE-FIELD BREAST TREATMENT TECHNIQUE WITH PRECISE GEOMETRIC MATCHING USING MULTILEAF COLLIMATOR-EQUIPPED LINEAR ACCELERATORS

XING-QI LU, Ph.D., STEPHANIE SULLIVAN, C.M.D., THOMAS EGGLESTON, B.S., R.T.(T), EDWARD HOLUPKA, Ph.D., MARC BELLERIVE, M.S., ANTONY ABNER, M.D., CAROLYN C. LAMB, M.D., ANITA LEE, M.D., MARY ANN STEVENSON, M.D., Ph.D., AND ABRAM RECHT, M.D.

Department of Radiation Oncology, Beth Israel Deaconess Medical Center, Harvard Medical School, Boston, MA

Purpose: Many authors have studied the problems associated with the three-field breast treatment, yet the proposed solutions present their own difficulties. This study presents a technique that overcomes these difficulties, reduces scatter to the contralateral breast, and improves setup reproducibility.

Methods and Materials: Patients are set up with both arms raised superiorly on a breast board. A precise field-match is achieved by rotating the couch and collimator of the tangents, while the supraclavicular field is half-beam blocked using an independent jaw. The posterior borders of the tangents are conformally defined by multileaf collimation. Measurements were performed to verify the field matching and evaluate scatter doses.

Results: A smooth dose transition was found at the match line at all depths. Corner blocks and lower wedges were not used, which reduced the scatter to the contralateral breast compared with our prior technique.

Conclusion: The technique achieves a precise match while removing constraints on the tangents' length and decreasing scatter dose. Procedures for simulation, planning, and treatment have been devised, along with a new patient setup routine incorporating orthogonal setup films and tattoos. This technique has been successfully implemented in routine treatment since September 2001. A program calculating the setup parameters is available at our website. © 2003 Elsevier Science Inc.

Breast cancer treatment, Irradiation of breast cancer, Three-field breast treatment.

## INTRODUCTION

Patients with breast cancer are often treated by a threefield technique, in which opposing tangential fields treat the breast or chest wall and lower axilla and a separate adjacent en-face field treats the upper axillary and supraclavicular region superiorly to the tangents. The complex geometry of this approach poses substantial technical challenges. Among them is the need to eliminate the geometric gaps and overlaps of the three fields both on the body surface and at depth. Several investigators (1–5) have described techniques that use a corner block to match the superior edges of the tangential fields to the half-beam blocked supraclavicular field and rely on collimator rotation to make the posterior border of the tangential fields parallel to the chest wall. Although widely used, its accurate implementation requires skillful work in making the corner block and daily check of the block position. As accelerators with multileaf collimators (MLC), such as the Varian 2100C/D and 21EX, have gained in popularity, new problems have arisen. For these machines, a lower wedge (i.e., one placed below the block tray) is used when a corner block is used. The increased length of the machine head plus these additional accessories causes the lower wedge to come very close to the patient. This not only increases the scatter dose but also makes it difficult to achieve proper setup of a patient who has both arms raised superiorly on a breast board

One possible solution to some of these problems is the single isocentric technique (6-8), which requires the use of half-beams blocks for both the supraclavicular and tangential fields. For a machine having asymmetric jaws and MLC, the longitudinal (y axis) jaws beam-split all three fields along the central plane with the MLC used to create the lung block (9). With this approach a geometrically perfect match is obtained and the corner block can be eliminated, so that an upper wedge can be used instead of a lower wedge. The absence of couch movement

Reprint requests to: Xing-Qi Lu, Ph.D., Department of Radiation Oncology, Beth Israel Deaconess Medical Center, Harvard Medical School, Boston, MA 02215. Tel: (617) 667-9564; Fax: (617) 667-9599; E-mail: xlu@bidmc.harvard.edu

mouth-Hitchcock Medical Center, 1 Medical Center Drive, Lebanon, NH 03756.

Received Jun 24, 2002, and in revised form Nov 20, 2002. Accepted for publication Nov 27, 2002.

<sup>&</sup>lt;sup>1</sup> Current address: Department of Radiation Oncology, Dart-

between fields also shortens the setup time. However, this technique also has its limitations (9). The main disadvantage is that it cannot be used for tangential field lengths greater than half of the maximum MLC opening, which is 20 cm even with the latest 120-leaf MLC Varian 21EX accelerator. This length is not adequate for a significant portion of patients. Another limitation of the single isocenter technique is that it results in a higher dose gradient for the supraclavicular field, due to the decreased source to skin distance (SSD).

Another technique that avoids the limitation on the tangential field length has been proposed, which beamsplits only the supraclavicular fields and uses a block to shield the lung (10). It has been assumed that the divergence of the non-beam-split tangential fields at the match line could be eliminated by angling the treatment couch alone. As pointed out by Siddon, this assumption is not true and a perfect match can only be achieved by simultaneously rotating the couch and the collimator (11). One approach along this direction has been proposed (12). However, we have found the formulae in this paper to be inaccurate, resulting in substantial mismatching between the lateral tangential and the supraclavicular fields. As shown in the Appendix, the angle between the superior borders of the two tangents can be as large as 10° based on the formulae. Realizing the difficulty in setting the collimator and turntable angle based on the formulae, it was suggested in the paper to use a collimator angle of 4° for 100-cm source to axis distance (SAD) setup. The turntable angle is then determined using fluoroscopy, matching the cephalad field border of the tangent to the supraclavicular wire. The problem of this empiric approach is that matching the cephalad field border of the tangent to the supraclavicular wire does not guarantee that the fields match below the skin surface. As demonstrated in the Appendix, the minimum mismatch between the superior borders of the two tangents can be larger than 4°. A precise solution for this supraclavicular-tangents beam match was described previously by Siddon (13, 14), in which a rotatable half-beam block was used. Although this method offered a number of advantages, the rotatable block was heavy and cumbersome. It was therefore soon replaced by the corner block method (1).

We present here an approach that has been implemented at Beth Israel Deaconess Medical Center in Boston. In this new approach, a precise geometric match in the vertical transverse plane is achieved by beam-splitting the supraclavicular field and rotating both the couch and the collimator for the tangential fields. The MLC is used to block the lung in a conformal fashion. Because a corner block is not needed, the lower wedge can be replaced by an upper wedge. This leaves more room between the collimator head and the patient, allowing easier patient setup. No limit is imposed on the field length, and the scatter dose to the contralateral breast and lung is reduced. A new setup routine has also been

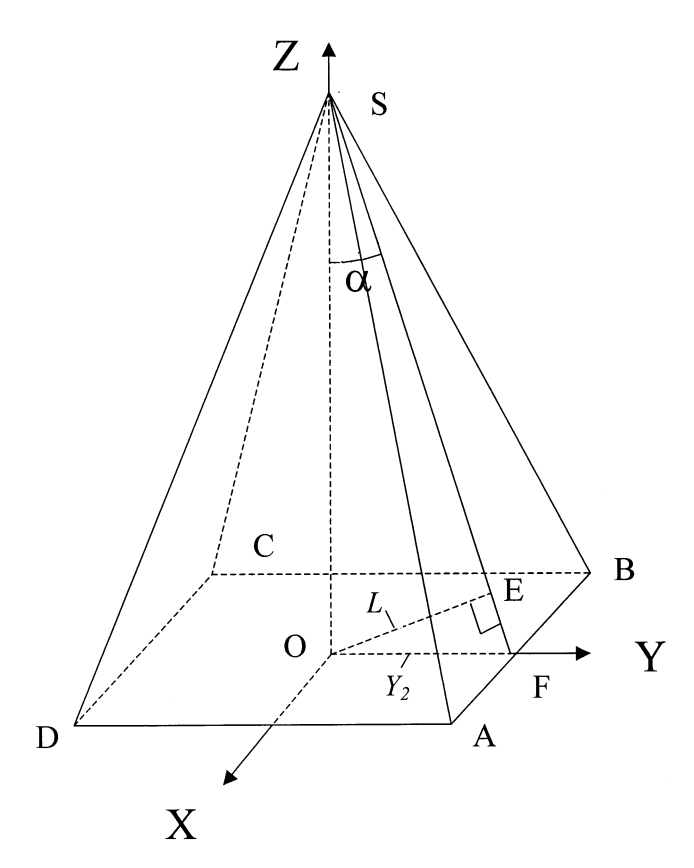


Fig. 1. The pyramid SABCD represents a beam field where collimator angle  $(\theta_c)$ , gantry angle  $(\theta_g)$ , and table angle  $(\theta_t)$  are all at  $0^\circ$  according to the IEC definition. The y axis is in the direction toward the gantry.

created to implement this approach and to reduce daily setup error, which includes the use of orthogonal setup fields.

# METHODS AND MATERIALS

Analytic analysis

In Fig. 1, the pyramid SABCD represents a beam field when collimator angle  $(\theta_c)$ , gantry angle  $(\theta_g)$ , and table angle  $(\theta_t)$  are all at  $0^\circ$  according to the International Electrotechnical Commission (IEC) definition. The coordinate system (x-y-z) axis) and its origin O, which is the isocenter, are fixed in space, whereas the beam source (S) can be rotated around the z axis and y axis. The plane SAB represents the superior border of the field. Vector  $O\vec{E}$  is perpendicular to plane SAB with a length of OE = L, and angle  $\alpha$  is defined as:

$$\alpha = \angle OSE = \sin^{-1}(L/100), \tag{1}$$

where OF is the upper half field length, defined as  $Y_2$ :

$$Y_2 = L/\cos\alpha,\tag{2}$$

which is only slightly larger than L in the clinically relevant situation.

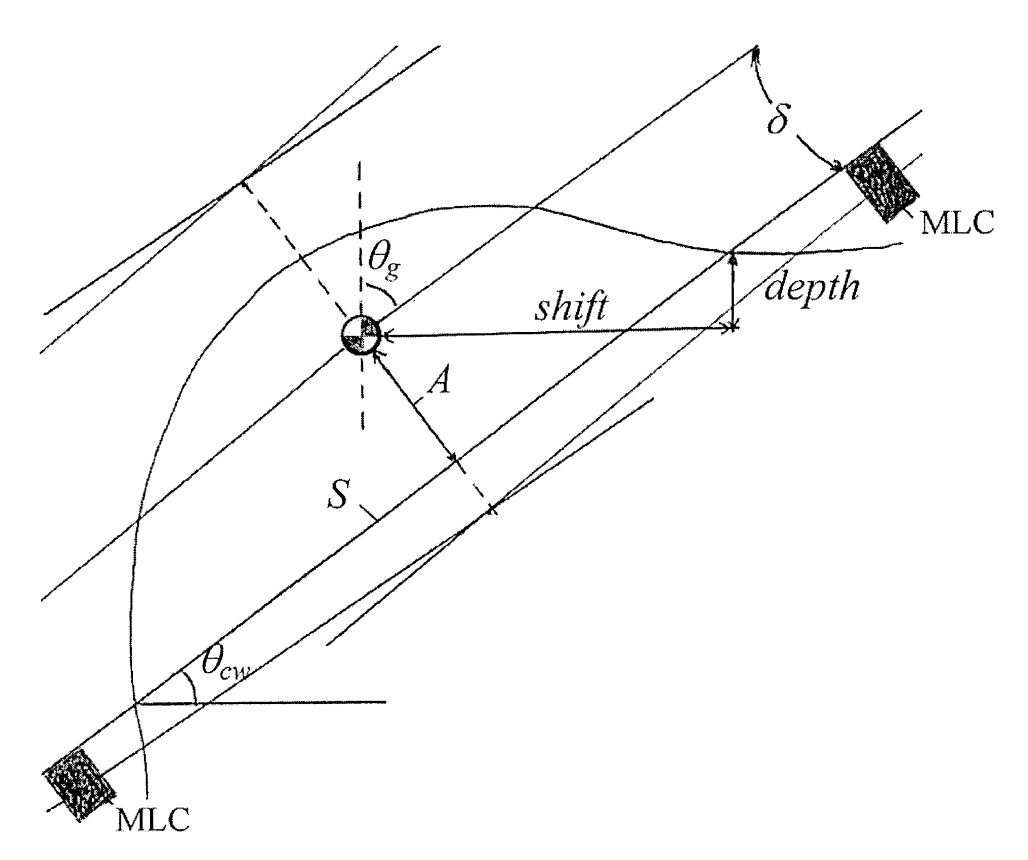


Fig. 2. The central transverse plane for a right breast, where S is the breast separation, A is the distance from the isocenter to the posterior border defined by MLC,  $\theta_{cw}$  is the chest wall angle, from which the gantry angle  $\theta_e$  for both tangents and the shift and depth can be determined with a condition that the posterior borders of the two tangents are coincident.

The collimator angle  $(\theta_c)$  and the table angle  $(\theta_t)$  for a tangential field with a given gantry angle  $(\theta_o)$  should be determined such that the superior border, plane SAB, matches precisely with the vertical transverse plane of the supraclavicular field, which is perpendicular to the y axis with a distance L to the isocenter (O). Once this is achieved, vector  $O\tilde{E}$  will become coincident with the y axis. Siddon had found the solution (14):

$$\theta_c = -\sin^{-1}(\tan\alpha/\tan\theta_o),\tag{3}$$

$$\theta_t = \sin^{-1}(\sin\alpha/\sin\theta_g). \tag{4}$$

We then need to determine the gantry angle  $(\theta_a)$  for both tangential beams, the vertical distance depth, and the lateral distance shift used for isocenter setup. To avoid added mathematical complexity at the beginning of the analysis, we first assume that both the collimator and the couch are not rotated. With this assumption, the parameters can be found easily in the central transverse plane in Fig. 2 in a condition that the posterior borders of the tangential fields are coincident in the central transverse plane:

$$Depth = (S/2)\sin\theta_{cw} - A\cos\theta_{cw},$$
  
$$Shift = (S/2)\cos\theta_{cw} + A\sin\theta_{cw},$$

$$\theta_{Rmg} = 90 - \vartheta_{cw} + \delta,$$

$$\theta_{Rlg} = 270 - \vartheta_{cw} - \delta,$$

$$\theta_{Lmg} = 270 + \vartheta_{cw} - \delta,$$

$$\vartheta_{Llg} = 90 + \vartheta_{cw} + \delta,$$
(5)

where  $\delta = \sin^{-1}(A/100)$ , S is the chest wall separation,  $\theta_{cw}$ is the chest wall angle,  $\theta_{Rmg}$  and  $\theta_{Rlg}$  are the right medial and lateral gantry angles,  $\theta_{Lmg}$  and  $\theta_{Llg}$  are the left medial and lateral gantry angles, and A is the distance from the isocenter to the posterior field edge defined by MLC, which in general is smaller than the half-width defined by the x jaws. A stringent analysis is presented in the Appendix, which demonstrates that the mismatch of the two posterior borders caused by the assumption in Eq. 5 is 0.1° or less, which is negligible.

For those interested, an easy-to-use calculation program of the parameters needed for the setup, comprised of Eqs. 1-5, is provided at the following website: http://spacely.jcrt.harvard.edu/Forms/BIDMC-Breast-Set-up.html.

The upper part of the table found at the website calculates the depth, lateral shift, and the gantry angle ( $\theta_{Rmg}$ ,  $\theta_{Rlg}$  or  $\theta_{Lmg}$ ,  $\theta_{Llg}$ ) for the tangential beams in a three-field plan. The

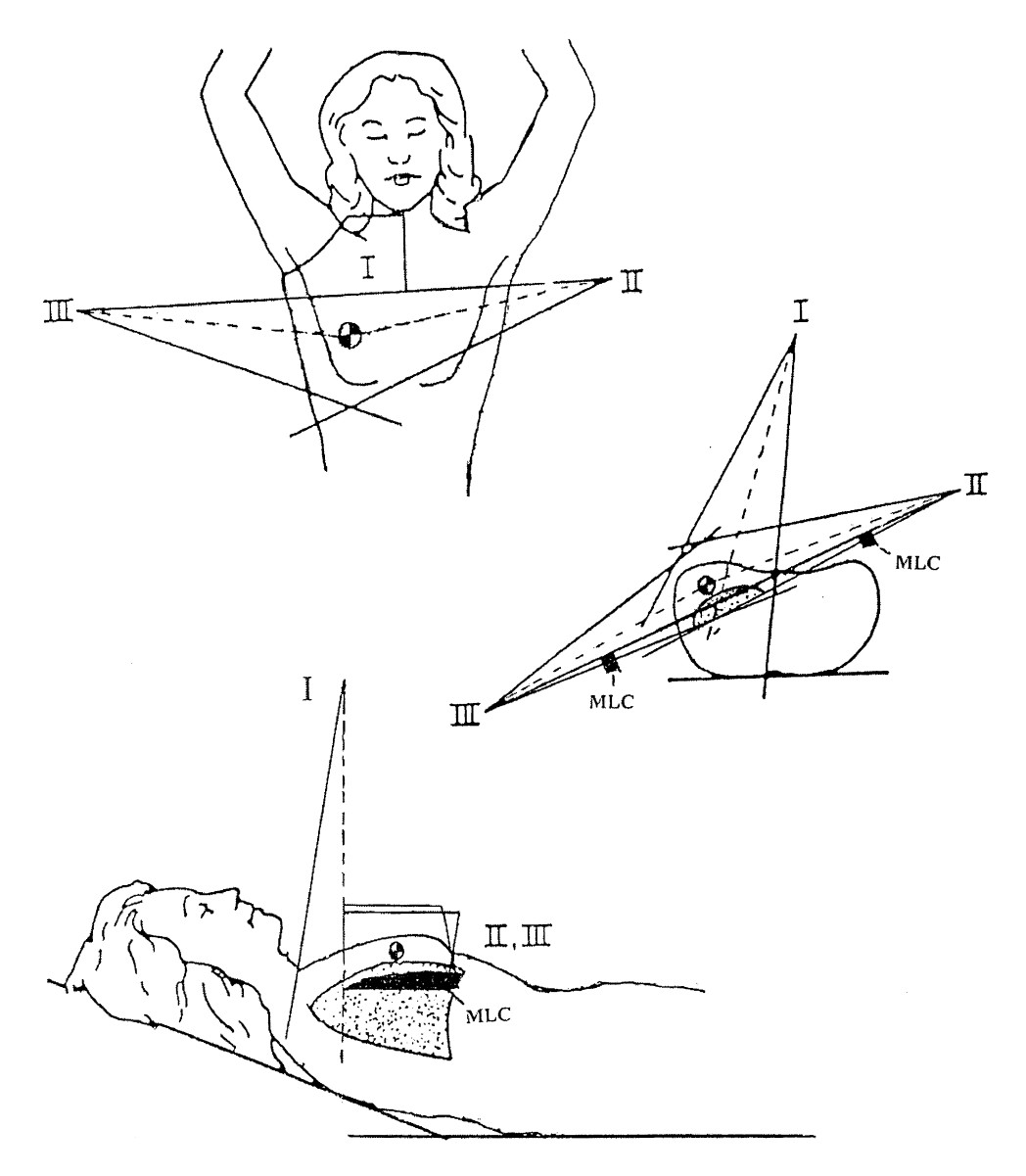


Fig. 3. The setup geometry; the treatment fields are indicated on the diagram as the (I) anterior supraclavicular, (II) medial tangential, and (III) lateral tangential fields.

simulator gantry angle  $(\theta_{sim})$  in the program, as explained in the patient setup procedure in the following subsection, is used to determine the chest wall angle  $(\theta_{cw})$ . The lower part of the table calculates  $Y_2$ , the collimator angle  $(\theta_c)$ , and the table angle  $(\theta_t)$  of the tangential beams for the three-field plan. The table also can be used when treatment of the axilla is supplemented with a smaller direct opposing posterior field (the four-field plan).

The setup geometry of the technique is demonstrated in Fig. 3, where the anterior supraclavicular field is blocked at the central axis using an independent jaw, and the posterior borders of the tangential beams are defined by MLC.

In the Appendix, parameters for two typical setup cases are calculated using this technique (Eqs. 3–5). They are also compared with those proposed previously (10, 12). These

calculations show the new technique results in a perfect geometric match, whereas there are significant mismatches using previous techniques.

# Match line verification and dosimetry

The results from the analytical analysis were verified by both geometric simulation and film dosimetry. Figure 4 shows the geometric simulation of the beam setting in three orthogonal views from a three-dimensional planning system. Both the sagittal and coronal views demonstrate a precise match between the supraclavicular to the tangential fields.

A solid water phantom was used to mimic a patient for the dosimetry study. The supraclavicular field was designed to deliver 100 cGy to the center for the field at a depth of 5 cm. The tangential fields were designed to

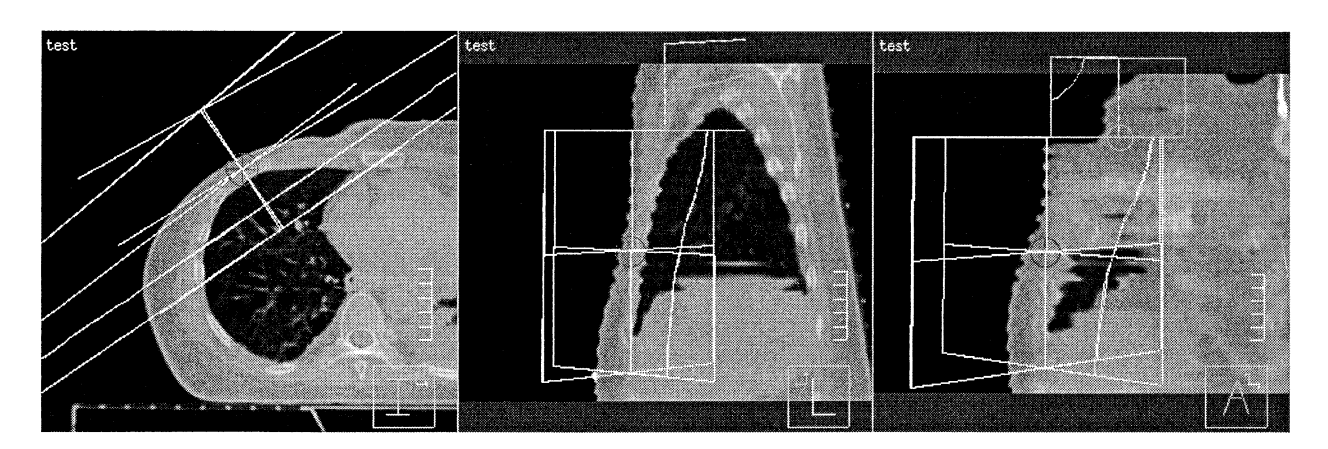


Fig. 4. A geometric simulation in the ADAC Pinnacle<sup>3</sup> planning system for a three-field treatment. The left figure is the transverse view in the central-axis plane of the tangential fields. The sagittal (the middle figure) and coronal (the right figure) views show a perfect match between the supraclavicular and tangential fields. The lines inside the tangential fields represent the mirror-flipped lung blocks. As shown in the sagittal and coronal views, the posterior edges as defined by the MLC leaves match quite well with each other.

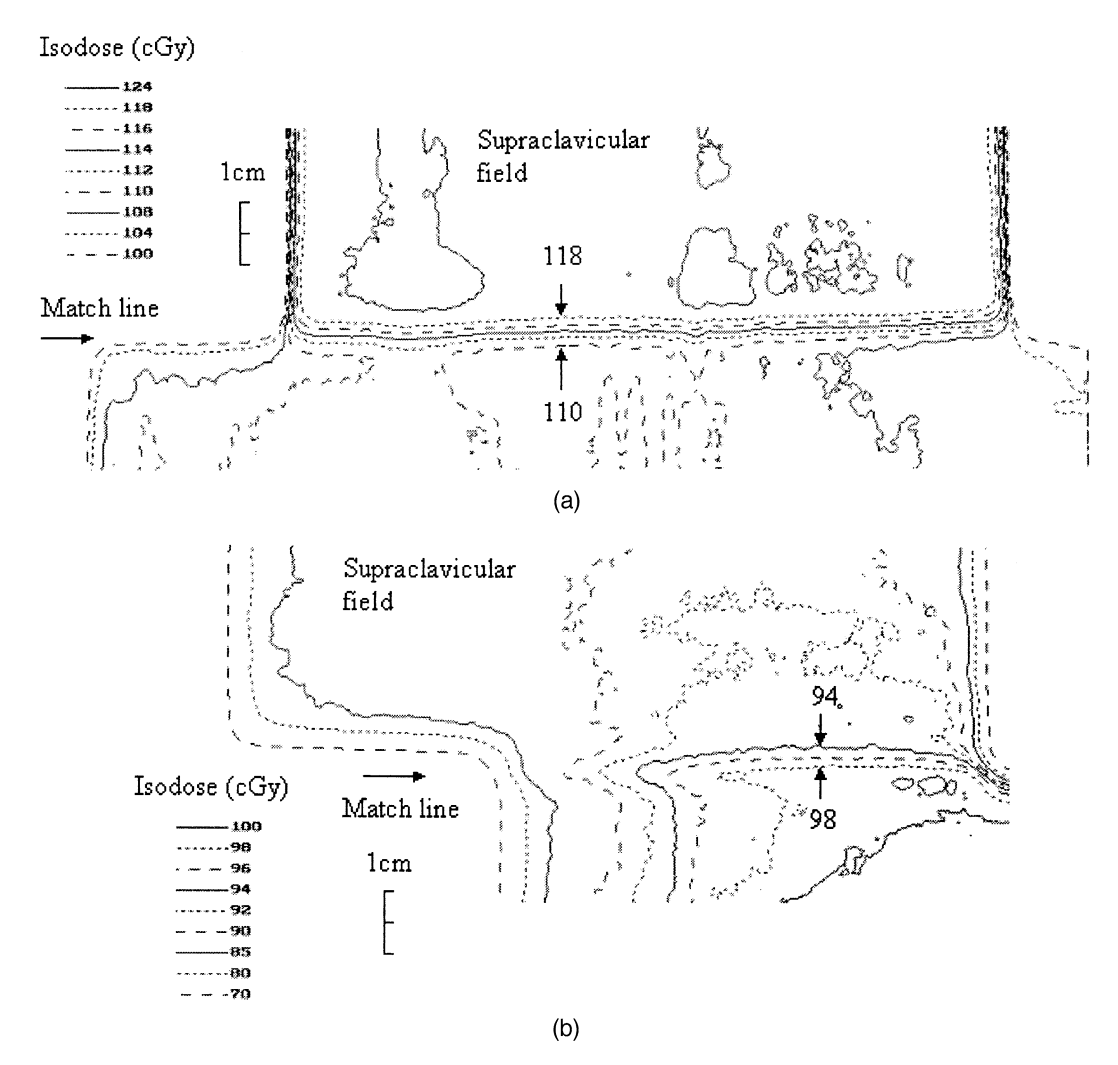


Fig. 5. (a) Isodose curve at depth of 1 cm from the film dosimetry. (b) Isodose curve at depth of 7 cm from the film dosimetry.

Medial field Lateral field Total dose Technique Depth (%) (%) (%) New Surface 8.2 1.8 10.0 2 cm 3.2 1.6 4.8 Old Surface 13.1 2.0 15.1

Table 1. Dose of contralateral breast at 5 cm from the midline

The doses measured 5 cm away from the midline are expressed as percentage of the dose to the normalization point in the central plane. The "New" technique is that presented in this paper, the "Old" technique refers to that using lower wedges and corner blocks.

1.9

4.3

deliver 100 cGy to the normalization point, which was 1.5 cm from the posterior edge of the treatment field at the mid-separation on the central-axis plane. Films were inserted at depths of 1 cm, 3 cm, 5 cm, and 7 cm. The isodose curve distributions at depth of 1 cm and 7 cm are shown in Fig. 5. A smooth dose transition between the tangential field region and the supraclavicular region is evident. The films taken at 3 cm and 5 cm demonstrate the same smooth transition.

2 cm

The dose to the contralateral breast, which may increase the risk of developing a contralateral breast cancer, has been studied by many authors (15-19). This dose varies substantially with different treatment conditions. With our approach, the dose to the contralateral breast and lung should be reduced, due to the use of the upper wedge and MLC instead of the corner block and the lower wedge. The dose to the contralateral breast measured with a phantom for the new method is shown in Table 1, compared with that from the "corner block/lower wedge" method. Thirty-degree wedges were used in both cases. A Varian 6-EX machine was used for this measurement. A Capintec surface chamber (PS-033) with a very thin window (mass attenuation thickness of 0.5 mg/cm<sup>2</sup>, 16.2 mm in diameter) was used to measure the dose. The gantry angles used for the breast treatment were 312° and 138° for the medial and the lateral fields, respectively. The center of the chamber was 5 cm away from the midline. The open field was 13 cm  $\times$  20 cm. In the new technique, the field size was defined by MLC with the jaw size set to 15(8.5, 6.5) cm  $\times$  20 cm for the medial and 15(6.5, 8.5) cm  $\times$  20 cm for the lateral; i.e., the MLC was set 2 cm inside the posterior jaw. For the "corner block/lower wedge" technique, the jaw size was  $13 \text{ cm} \times 22 \text{ cm}$  with a corner block in the superior side; i.e., the corner block was set 2 cm inside the superior jaw. The doses measured 5 cm from the midline at the surface and at a depth of 2 cm are presented as a percentage of the dose to the normalization point. The results show a significant dose reduction to the contralateral breast using the new method, i.e., about one-third reduction at the surface and one-fourth reduction at a depth of 2 cm. This result varied little when wedges other than 30° were used.

The dose to the ipsilateral lung was measured with film dosimetry for the same treatment parameters described in the last paragraph. The dose distributions on the line perpendicular to the posterior field edge passes through the normalization point are shown in Fig. 6 (with an uncertainty of  $\pm 3\%$  in dose and  $\pm 1$  mm in position). It was observed that the dose using the new method is slightly higher than that with the "corner block and lower wedge" technique in the penumbra region due to the transmission through the MLC (approximately 1.4%). However, at depths deeper than approximately 1 cm, the new technique resulted in lower doses. For depths below 2 cm, the dose using the new method was about 20% or more lower than the "corner block and lower wedge" technique. Spot check of the doses by ion chamber measurement was consistent with the film dosimetry.

6.2

Patient setup technique utilizing both conventional fluoroscopic and computed tomography (CT) simulation

The patient is first placed in position on a two-arm breast board with verification of proper positioning under fluoroscopy on the conventional simulator. The central axis is placed over the midline and marked.

To simulate the half-beam blocked supraclavicular/ axillary field, the central axis is placed at the inferior aspect of the clavicular head at a distance of 100 SSD. The gantry is then angled approximately 10° toward the contralateral breast with the medial field edge splitting the suprasternal notch and the lateral field edge placed to include the proximal two-thirds of the humeral head (for a full axillary field) or at the coracoid process (for a supraclavicular field). The superior border is placed at the superior-most aspect of the first rib. The field borders are fine-tuned during fluoroscopy and a film is taken. The gantry is brought back to the vertical, and the central-axis point ("point A") and the medial setup edge point ("point B") are marked (Fig. 7). An off-axis distance is recorded in the supraclavicular fossa, because this is the site of interest. The table is unlocked, and the central axis is moved to the supraclavicular fossa, where the SSD is recorded.

Proceeding to the tangents, a helically coiled double marking wire is clinically placed by the physician to show the desired position of the medial border of tissue to be treated. Likewise, a single-stranded wire is placed to mark the desired lateral border of the tissue to be treated. A

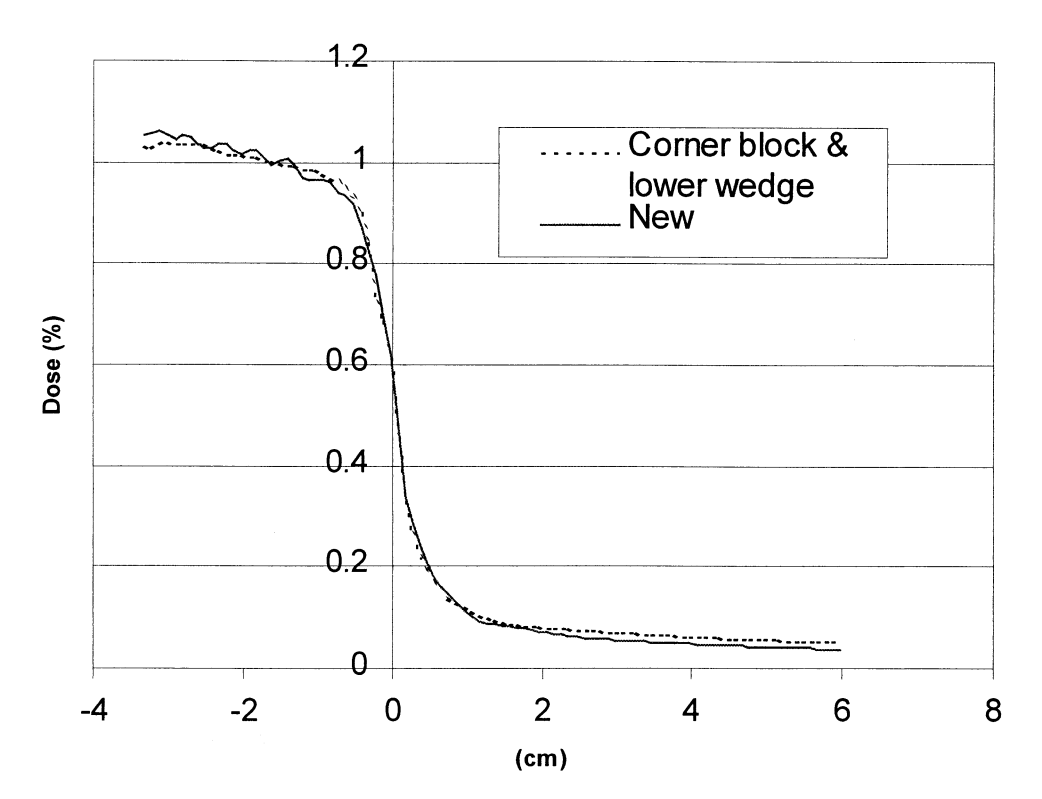


Fig. 6. The dose distributions in the line perpendicular to the chest wall passing through the normalization point, which is at x = -1.5 cm. Field edge is at x = 0 cm. The "corner block and lower wedge" technique is compared with the new technique proposed here.

radiopaque marker ("BB") is placed approximately 1.0–2.0 cm inferior to the inframammary fold, and another radiopaque marker is placed on the vertical center of the supraclavicular match line (point A in Fig. 7).

With the gantry at vertical, the central axis is placed on the medial marker wire. The patient is placed at 100 SSD at the central axis. The couch vertical and couch lateral readings are recorded from the simulator monitor. The field length is initially established by opening the field to match superiorly the radiopaque markers placed on the matchline and inferiorly at the inframammary fold. The gantry is rotated under fluoroscopic guidance until the medial and lateral wires intersect; the gantry angle  $(\theta_{sim})$ is then recorded. This angle ( $\theta_{sim}$ ), along with the tangent separation between the two wires (S) and the distance (A), which is taken as half of the estimated field width necessary to encompass the breast in the central transverse plane, are entered into the upper table of the website setup program. This yields the vertical distance depth (depth), the lateral distance shift (shift), and the gantry angle setup for both tangential fields ( $\theta_{Rmg}$ ,  $\theta_{Rlg}$  or  $\theta_{Lmg}$ ,  $\theta_{Llg}$ ). The chest wall angle is also given in the table, which is determined by  $\theta_{cw} = 90 - \vartheta_{sim}$  for the right breast,  $\theta_{cw} = \vartheta_{sim} - 270$  for the left breast. The distance from the isocenter to the supraclavicular transverse plane (L) is then measured and entered into the table, which gives the upper half field length  $(Y_2)$ , the collimator angle  $(\theta_c)$ , and the table angle  $(\theta_t)$  for both tangential beams.

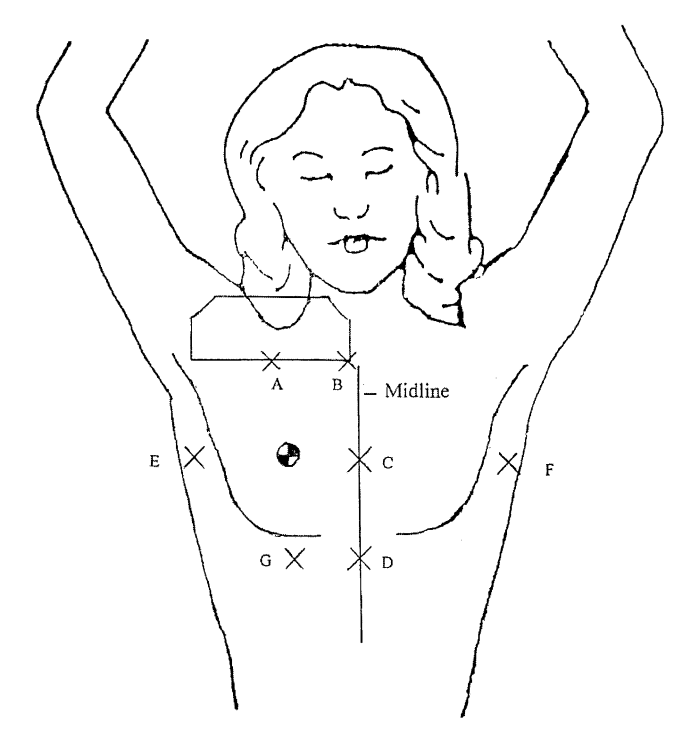


Fig. 7. The seven tattooed setup points (A–G). Points C, D are for straightening and points E, F for leveling the patient. Points A, B are for the supraclavicular field setup. Point C is also for localizing the isocenter for the tangential fields, and point G is for the isocenter verification.

All of these calculated parameters are then implemented at the simulator. The calculated parameters are verified at the simulator, demonstrating that the superior edge of both the medial and lateral tangents fall exactly along the match-line. The field width, started as 2A, is then opened symmetrically or independently to cover a triangle of tissue in the superior-posterior edge while leaving enough flash at the anterior border.

Once the setup is acceptable, the medial and lateral tangent films are taken. The medial wire and the lateral wire should be superimposed (as they were during the fluoroscopic portion of the simulation). If an unacceptable volume of lung was included in the field, the wires can be relocated and the breast program is repeated with the modified field edges. Finally, lateral and anterior orthogonal setup films are taken, with the modified field blades opened sufficiently to expose the vertebral bodies. The vertebral bodies serve as the critical landmarks when portal films of these orthogonal films are taken, because the ribs and other structures of the chest move with respiration.

To complete the setup, the following seven points are tattooed, as indicated in Fig. 7: Point A, the central-axis point on the matchline; Point B, the medial setup edge point on the matchline; Point C, the intersection of the isocenter plane at midline; Point D, the inferior central axis of the field at midline; Point E, the intersection of the isocenter plane at the lateral field edge; Point F, the opposed leveling point on the contralateral chest wall; Point G, the inferior central axis over the breast.

A setup photograph of the patient's position and the breast board settings are recorded, along with a single digital contour performed along the isocenter plane. The vertical depth and the lateral shift relative to Point C are also recorded for later setup. These numbers can be different from the *depth* and *shift* from the calculation program, which are relative to the medial entry-point in the isocenter plane.

If desired, CT simulation may be performed with the patient in the same setup with a radiopaque marker denoting each tattoo. This allows more precise blocking of the lung and heart or inclusion of the internal mammary nodes, should the physician wish to treat them. The blocks can be appropriately modified from those obtained using fluoroscopic simulation.

In some patients, a portion of the axillary tail of the breast may be located outside the tangential fields. For patients undergoing conventional (fluoroscopic) simulation, the physician examines the light-field projection of the supraclavicular field and decides whether to extend the supraclavicular field to cover the breast superolaterally, based on his or her clinical judgment. This procedure is the same as when our prior technique was used. When CT-guided planning is performed, the entire periphery of the breast is outlined by wire, and thus the CT images may be used by the physician in making this decision.

Planning and treatment

After the simulation, the data including block positions are first transferred to a treatment planning system. The isocenter is localized using fiducial markers along with the depth and the lateral shift. The setting is then verified by comparing the orthogonal digitally reconstructed radiographs and the simulation films. The geometric match is visually checked by a three-dimensional view, as shown in Fig. 4. The lung, heart, and tumor bed volumes and internal mammary nodes are outlined, as needed.

The preliminary plan is evaluated based on the dose distribution and the dose-volume histograms. If the plan has to be modified (for instance, when the physician decides that heart/lung volumes involved are excessive, and therefore the gantry angle or the posterior field border need to be adjusted), all the setup parameters may be changed without repeating the simulation. However, we prefer to keep the distance shift unchanged, so that the point G is always valid in the isocenter setup. As indicated in Eq. 6, the lateral distance shift is determined by the chest wall angle  $\theta_{c,w}$ , the separation S, and distance A. If  $\theta_{c.w.}$  and/or S have to be changed from the initial values, one can vary the distance A to maintain the initial value of the shift, which can be done easily with the program. Finally, in the setup sheets for treatment, the values for angle (in degree) and distance (in cm) are specified to one digit after the decimal point.

For treatment, the patient is placed on a two-arm breast board as for the simulation. All seven tattoos are identified. Four-point setup tattoos (points C–F) are used for both straightening and leveling the patient. The supraclavicular field is set up based on points A and B, and the matchline is drawn on the skin. For the tangential beam setup, when the distance shift is performed properly, then the central axis at isocenter will match tattoo G, and the superior border will be coincident with the match line. Stringent tolerances (0.5° for all angles, and 0.3 cm for the table longitudinal setting) are imposed on the treatment setup.

### DISCUSSION

The technique presented in this study provides several advantages over the corner block technique. By rotating both the couch and the collimator for the tangential fields, the match of the supraclavicular field to the tangential fields is made geometrically precise. The corner block is eliminated. An upper wedge may be used instead of a lower wedge, which eliminates the difficulties in setting up the medial field due to the gantry head coming too close to the patient (for machines such as Varian 2100 C/D and 21EX). Patients may be positioned with both arms up on the breast board, which helps to eliminate patient rotation and provides a more reproducible setup. The posterior field edge for the tangents is defined by the MLC, so that the MLC leaves can be shaped to better protect the lung and heart rather than a straight line as with the corner block technique. Because there is less scatter dose from the upper wedges than from lower wedges and the MLC effectively blocks much of the scatter dose originating from the jaws, this new technique also reduces the dose to the contralateral breast and the ipsilateral lung. Furthermore, intensity-modulated radiotherapy to the breast can easily be implemented as a part of three-field breast treatment using this approach. Compared with the single isocentric technique, the main advantage of this approach is that the tangential field length is no longer a limiting factor (even for machines with 52-leaf MLC).

Achieving coplanarity of the posterior field edges is another desirable goal in three-field treatment. The gantry angles of the tangential beams, determined in Eq. 5, result in the posterior edges of the two tangents being precisely coincident on the central transverse plane. Because the distance between the central axis and the posterior edge (distance *A* in Eq. 5) varies in different transverse planes along the entire length of the tangential beams (to better protect the lung and heart), this coincidence cannot always be maintained in the noncentral transverse planes. However, this mismatch is small. As shown in the sagittal and coronal views in Fig. 4, where two blocks (MLC) are mirror-flipped between the tangents, the match of the posterior edges of the two tangential field is quite good.

The seven tattooed points are located in places on the body that are generally firm and not easily displaced once a patient is on the breast board. Therefore, we find that placing these tattoos saves time during patient setup on treatment, although the added tattoos slightly increase the length of simulation. Basing setup on these points, in combination with the use of orthogonal setup films, greatly improves patient setup. Fields can be adjusted if

desired without needing to reposition these setup points. This allows more flexibility in postsimulation planning.

The planning time of the current technique is slightly longer than that for the corner block technique we previously used, but the current technique is much more flexible. There is no need to resimulate and change the marks on the patient if the setup has to be modified. Construction of the corner block and the daily checking of its position are eliminated. Treatment delivery takes less time, and its reproducibility is improved significantly, with fewer setup corrections required in the new technique compared with the old one.

Techniques have been proposed (12, 20) to use half-beam to create the posterior border for the tangential fields. One may accommodate these techniques to this proposed approach. The posterior edge needs to be opened in this approach, so that MLC can be used to define the border conformally. This ensures a precise match of the posterior borders in the midplane and simplifies the calculation formulae, but dynamic wedges may be needed, which requires more quality assurance checking than with fixed wedges.

In conclusion, a beam matching technique for three-field breast treatment has been developed and thoroughly tested. Over 100 patients have been treated since September 2001 with this technique. A precise geometric match in the vertical transverse plane is obtained by beam-splitting the supraclavicular field and rotating both the couch and the collimator for the tangential fields. By defining the posterior borders of the tangential fields using MLC, this technique eliminates the use of the corner block and the lower wedge, which avoids setup problems due to close approach of the accelerator head to the patient, reduces the scatter dose to both the ipsilateral lung and contralateral breast, and eliminates limitations on the tangential field length.

## REFERENCES

- Sidddon RL, Buck BA, Harris JR, et al. Three-field technique for breast irradiation using tangential field corner blocks. Int J Radiat Oncol Biol Phys 1983;9:583–588.
- Lichter AS, Fraass BA, van de Geijin JA. Technique for field matching in primary breast irradiation. *Int J Radiat Oncol Biol Phys* 1983;9:263–270.
- Lebesque JV. Field matching in breast irradiation: An exact solution to a geometrical problem. *Radiother Oncol* 1986;4: 47–57
- Hunt MA, Kutcher GJ, Martel MK. Matchline dosimetry of a tree field technique for breast treatment using Cobalt or 6 MV X rays. *Int J Radiat Oncol Biol Phys* 1987;13:1099–1106.
- Chu JCH, Solin IJ, Hwang CC, Fowble B, Hanks GE, Goodman RI. A nondivergent three field matching technique for breast irradiation. *Int J Radiat Oncol Biol Phys* 1990;19:1037– 1040
- 6. Podgorsak EB, Gosselin M, Pla M. A simple isocentric technique for irradiation of the breast, chest wall and peripheral lymphatics. *Br J Radiol* 1984;37:57–63.
- Conte G, Nascimben O, Turcato G, et al. Three-field isocentric technique for breast irradiation using individualized shielding blocks. Int J Radiat Oncol Biol Phys 1988;14:1299

  1305.

- Rosenow UF, Valentine ES, Davis LW. Technique for treating local breast cancer using a single set-up point and asymmetric collimation. *Int J Radiat Oncol Biol Phys* 1988;14:1299– 1305
- Klein LE, Taylor M, Michaletz-Lorenz M, Zoeller D, Umfleet W. A mono isocentric technique for breast and regional nodal therapy using dual asymmetric jaws. *Int J Radiat Oncol Biol Phys* 1994;28:753–760.
- Bedwinek J. Treatment of stage I and II adenocarcinoma of the breast by tumor excision and irradiation. *Int J Radiat* Oncol Biol Phys 1981;7:1553–1559.
- Siddon RL. Letter to the editor. Int J Radiat Oncol Biol Phys 1984;10:1817–1818.
- Hartsell WF, Murthy AK, Kiel KD, Kao M, Hendrickson FR. Technique for breast irradiation using custom blocks conforming to the chest wall contour. *Int J Radiat Oncol Biol Phys* 1990;19:189–195.
- Siddon RL. Tonnesen GL, Svensson GK. Three-field technique for breast irradiation using a rotatable half-beam block. *Int J Radiat Oncol Biol Phys* 1981;7:1473–1477.
- Siddon RL. Solution to treatment planning problems using coordinate transformations. *Int J Radiat Oncol Biol Phys* 1981:8:766–774.

- Fraass BA, Roberson PL, Lichter AS. Dose to the contralateral breast due to primary breast irradiation. *Int J Radiat Oncol Biol Phys* 1985;11:485–497.
- Tercilla O, Krasin F, Lawn-Tsao L. Comparison of contralateral breast doses from ½ beam block and isocentric treatment techniques for patients treated with primary breast irradiation with 60 CO. Int J Radiat Oncol Biol Phys 1989;17:205–210.
- Kelly CA, Wang XY, Chu JC, Hartsell WF. Dose to the contralateral breast: A comparison of four primary breast irradiation techniques. *Int J Radiat Oncol Biol Phys* 1996;34:727–732.
- Weides CD, Mok EC, Chang WC, Findley DO, Shostak CA. Evaluating the dose to the contralateral breast when using a dynamic wedge versus a regular wedge. *Med Dosim* 1995;4:287– 293.
- Brooks PS. Dose to contralateral breast—a comparative study. *Med Dosim* 1995;4:301–307.
- Butker EK, Helton DJ, Keller JW, Jughes LL, Crenshaw T, Davis LW. A total integrated simulation technique for threefield breast treatment using a CT simulator. *Int J Radiat Oncol Biol Phys* 1996;23:1809–1814.

## **APPENDIX**

As described in "Methods and Materials," vector  $\vec{OE}$  in Fig. 1 is perpendicular to plane SAB with a length of OE = L, and can be used to represent plane SAB. For simplicity, we assume  $\vec{OE}$  is a unit vector, i.e., L = 1:

$$\vec{OE} = \begin{pmatrix} 0 \\ \cos(\alpha) \\ \sin(\alpha) \end{pmatrix}$$

The purpose is to determine the direction of vector  $O\tilde{E}$  when the collimator is rotated by an angle  $\theta_c$  and the table is rotated by an angle  $\theta_t$  for a tangential field with a given gantry angle  $\theta_g$ . To do this, we first rotate the beam pyramid around the z axis, i.e., to rotate the collimator, by angle  $\theta_c$ . The vector  $O\tilde{E}$  becomes:

$$O\vec{E}_c = \begin{pmatrix} \cos\theta_c & -\sin\theta_c & 0\\ \sin\theta_c & \cos\theta_c & 0\\ 0 & 0 & 1 \end{pmatrix} \begin{pmatrix} 0\\ \cos\alpha\\ \sin\alpha \end{pmatrix}$$
$$= \begin{pmatrix} -\sin\theta_c \cdot \cos\alpha\\ \cos\theta_c \cdot \cos\alpha\\ \sin\alpha \end{pmatrix}$$

Second, we rotate the beam pyramid around the y axis (i.e., to rotate the gantry) by a gantry angle  $\theta_g$ . The vector becomes:

$$\begin{split} O\vec{E}_{cg} &= \left( \begin{array}{ccc} \cos\theta_g & 0 & \sin\theta_g \\ 0 & 1 & 0 \\ -\sin\theta_g & 0 & \cos\theta_g \end{array} \right) \cdot \left( \begin{array}{c} -L \cdot \sin\theta_c \cdot \cos\alpha \\ \cos\theta_c \cdot \cos\alpha \\ \sin\alpha \end{array} \right) \\ &= \left( \begin{array}{ccc} -\cos\theta_g \cdot \sin\theta_c \cdot \cos\alpha + \sin\theta_g \cdot \sin\alpha \\ \cos\theta_c \cdot \cos\alpha \\ \sin\theta_g \cdot \sin\theta_c \cdot \cos\alpha + \cos\theta_g \cdot \sin\alpha \end{array} \right) \end{split}$$

Finally, we rotate the beam pyramid around the z axis again by angle  $\theta_r$ . This operation is equivalent to rotating the table according to the IEC definition by angle  $\theta_r$ . The vector becomes  $O\vec{E}_{cgt}$  as shown in Eq. 6.

Based on Eq. 6, the match of the superior border of the tangential fields to the vertical plane of the supraclavicular field can be verified. Substitute Eqs. 3 and 4 into Eq. 6, the components in the x and z axis become zero, and the y axis component is 1, which indicates a perfect match.

This is, however, not the case for the approaches proposed in Refs. 10 and 12. To quantitatively estimate the mismatches, we assume vector  $\vec{M}$  and  $\vec{L}$  are the vectors corresponding to the medial and the lateral field obtained in Eq. 6,  $M_x$ ,  $M_y$ ,  $M_z$  and  $L_x$ ,  $L_y$ ,  $L_z$  are the components in x, y, and z directions for  $\vec{M}$  and  $\vec{L}$ , respectively. The mismatch angles between the superior board of the tangential fields and the vertical plane of the supraclavicular field can be found as  $\cos^{-1}(M_y)$  and  $\cos^{-1}(L_y)$ . The mismatch angle between the superior boards of the two tangential fields is  $\cos^{-1}(M_xL_x+M_yL_y+M_zL_z)$ . In Table 2, these angles are quantitatively evaluated with two typical setup samples for those approaches discussed here.

The study by Bedwinek (10), labeled as technique "A" in Table 2, assumed that the divergence of the non–beam-split

$$O\vec{E}_{cgt} = \begin{pmatrix} \cos\theta_t & -\sin\theta_t & 0 \\ \sin\theta_t & \cos\theta_t & 0 \\ 0 & 0 & 1 \end{pmatrix} \cdot \begin{pmatrix} -\cos\theta_g \cdot \sin\theta_c \cdot \cos\alpha + \sin\theta_g \cdot \sin\alpha \\ \cos\theta_c \cdot \cos\alpha \\ \sin\theta_g \cdot \sin\theta_c \cdot \cos\alpha + \cos\theta_g \cdot \sin\alpha \end{pmatrix}$$

$$= \begin{pmatrix} -\cos\theta_t \cdot \cos\theta_g \cdot \sin\theta_c \cdot \cos\alpha + \cos\theta_t \cdot \sin\theta_g \cdot \sin\alpha - \sin\theta_t \cdot \cos\theta_c \cdot \cos\alpha \\ -\sin\theta_t \cdot \cos\theta_g \cdot \sin\theta_c \cdot \cos\alpha + \sin\theta_t \cdot \sin\theta_g \cdot \sin\alpha + \cos\theta_t \cdot \cos\theta_c \cdot \cos\alpha \end{pmatrix}$$
(6)
$$= \begin{pmatrix} \sin\theta_t \cdot \cos\theta_g \cdot \sin\theta_c \cdot \cos\alpha + \sin\theta_t \cdot \sin\theta_g \cdot \sin\alpha - \sin\theta_t \cdot \cos\theta_c \cdot \cos\alpha \\ -\sin\theta_t \cdot \cos\theta_g \cdot \sin\theta_c \cdot \cos\alpha + \sin\theta_t \cdot \sin\theta_g \cdot \sin\alpha + \cos\theta_t \cdot \cos\theta_t \cdot \cos\alpha \end{pmatrix}$$
(6)

Table 2. Comparison of the four matching techniques

Breast	Chest wall angle (°)	S (cm)	A (cm)	L (cm)	<i>Y</i> 2 (cm)	Field	Gantry (°)	Technique	Collimator (°)	Table (°)	Mismatch (°)
						Medial	52.3	A	0.0	5.1	3.3/7.1
Right	40	20	4	9.0	9.0			В	351.6	5.1	5.3/9.5
								C	356	6.5	0.0/0.6
								New	356.0	6.5	0.0/0.0
						Lateral	227.1	A	0.0	354.8	3.8/7.1
								В	352.5	354.8	4.3/9.5
								C	356	353.5	0.6/0.6
								New	355.2	352.9	0.0/0.0
						Medial	312.1	A	0	353.1	4.9/10.5
Left	45	20	5	12.0	12.1			В	10.1	353.2	5.8/10.4
								C	4	352.2	1.7/4.1
								New	6.3	350.7	0.0/0.0
						Lateral	137.9	A	0.0	6.9	5.6/10.5
								В	9.2	6.9	4.7/10.4
								C	4	7.6	2.4/4.1
								New	7.7	10.3	0.0/0.0

The "New" technique is that presented in this article. Technique "A" refers to the technique in Ref. 10, technique "B" refers to that based on the formulae in Ref. 12, and technique "C" refers to the best results one can achieve based on the empirical approach in Ref. 12. The first number under "Mismatch" is the angle between the superior border of the tangential field and the inferior border of the supraclavicular field; the second number is the angle between the superior borders of the two tangents.

tangential fields at the match line could be eliminated by angling the treatment couch alone, i.e.,

$$\theta_c = 0 \tag{7}$$

$$\theta_t = \tan^{-1}(L/100)$$
 (8)

In the second paper (12) it was suggested that a good match can be achieved when

$$\theta_c = \tan^{-1}(L/(100 \cdot \cos \vartheta_p)) \tag{9}$$

$$\theta_t = \tan^{-1}(L/100) \tag{10}$$

Notice the definition L here is the half field length, whereas in the study by Hartsell *et al.* (12) L is defined as the full length. The result for this approach is labeled as technique "B" in Table 2. In both techniques (A and B), the mismatch between the two tangents can be as large as  $10^{\circ}$ .

Due to the difficulty in setting the collimator and turntable angle in using Eqs. 9 and 10, the authors then suggested to empirically use a collimator angle of 5° for 80-cm SAD setup and 4° for 100-cm SAD setup and to determine the turntable angle using fluoroscopy, matching the cephalad field border of the tangents with the supraclavicular wire. To verify the accuracy, we can mathematically determine the best possible match, i.e., the minimum mismatch

angles, that can be achieved in this empiric approach by a condition:

$$\frac{dM_y}{d\vartheta_t} = 0$$

and

$$\frac{dL_{y}}{d\vartheta_{t}}=0,$$

from which the optimal table angle for the tangents is found:

$$\vartheta_t = \tan^{-1} \left( \frac{\sin \vartheta_g * \sin \alpha - co \vartheta_g * \sin \vartheta_c * \cos \alpha}{\cos \vartheta_c * \cos \alpha} \right)$$

The results, which are the best one can achieve, are labeled as technique "C" in Table 2. It is found that although the three field borders can sometimes be coincident within about 0.5°, the mismatch also can be as large as 4° even with the best effort.

Next, we will discuss Eq. 5, which is a simplified solution assuming that the collimator and table are not rotated. In Fig. 1, plane SAD is the posterior border for the right medium field and plane SBC is the posterior border for the right lateral. The distances from the isocenter (O) to these two planes are both equal A, which is shown in Fig. 2. Assuming A = 1, the vectors from O perpendicular to the planes before the collimator, gantry, and table rotation are:

$$\vec{A}_{med} = \begin{pmatrix} \cos \delta \\ 0 \\ \sin \delta \end{pmatrix}$$

and

$$\vec{A}_{lat} = \begin{pmatrix} -\cos\delta \\ 0 \\ \sin\delta \end{pmatrix}.$$

After the collimator, gantry, and table are rotated according to Eqs. 3–5, they become:

The angle between the two posterior borders, therefore, can be determined as  $COS^{-1}(\vec{A}'_{med}\cdot\vec{A}'_{lat})$ . Using the solution in Eq. 5 for the samples in Table 2, the mismatch angle is found to be  $0.1^{\circ}$  or less, which is negligible. Therefore, one may reasonably use Eq. 5 to avoid the very complicated result that follows from strict application of  $COS^{-1}(\vec{A}'_{med}\cdot\vec{A}'_{lat})=0$ .

$$\vec{A'}_{med} = \begin{pmatrix} \cos\vartheta_{t}\cos\vartheta_{rmg}\cos\vartheta_{c}\cos\delta + \cos\vartheta_{t}\sin\vartheta_{rmg}\sin\delta - \sin\vartheta_{t}\sin\vartheta_{c}\cos\delta \\ \sin\vartheta_{t}\cos\vartheta_{rmg}\cos\vartheta_{c}\cos\delta + \sin\vartheta_{t}\sin\vartheta_{rmg}\sin\delta + \cos\vartheta_{t}\sin\vartheta_{c}\cos\delta \\ - \sin\vartheta_{rmg}\cos\vartheta_{c}\cos\delta + \cos\vartheta_{rmg}\sin\delta \end{pmatrix}$$

and

$$\vec{A}'_{lat} = \begin{pmatrix} -\cos\vartheta_t\cos\vartheta_{rlg}\cos\vartheta_c\cos\delta + \cos\vartheta_t\sin\vartheta_{rlg}\sin\delta + \sin\vartheta_t\sin\vartheta_c\cos\delta \\ -\sin\vartheta_t\cos\vartheta_{rlg}\cos\vartheta_c\cos\delta + \sin\vartheta_t\sin\vartheta_{rlg}\sin\delta - \cos\vartheta_t\sin\vartheta_c\cos\delta \\ \sin\vartheta_{rlg}\cos\vartheta_c\cos\delta + \cos\vartheta_{rlg}\sin\vartheta \end{pmatrix}$$